PHYSICAL REVIEW B **71**, 241309(R) (2005)

Photovoltaic and rectification currents in quantum dots

M. G. Vavilov,[1,*] L. DiCarlo,[2] and C. M. Marcus[2]
[1]*Center for Materials Sciences and Engineering, Massachusetts Institute of Technology, Cambridge, Massachusetts 02139, USA*
[2]*Department of Physics, Harvard University, Cambridge, Massachusetts 02138, USA*
(Received 25 April 2005; published 15 June 2005)

We investigate theoretically and experimentally the statistical properties of dc current through an open quantum dot subject to ac excitation of a shape-defining gate. The symmetries of rectification current and photovoltaic current with respect to applied magnetic field are examined. Theory and experiment are found to be in good agreement throughout a broad range of frequency and ac power, ranging from adiabatic to nonadiabatic regimes.

DOI: 10.1103/PhysRevB.71.241309 PACS number(s): 73.23.−b, 73.40.Ei, 73.50.Pz

Transport in mesoscopic systems subject to time-varying fields combines elements of nonequilibrium physics and quantum chaos. This combination extends the scope of mesoscopic physics and is likely to be important in quantum information processing, where fast gating and quantum coherence are both required. Of particular importance is the ability to control external fields applied to the mesoscopic system and to distinguish effects of these fields on quantum dynamics of the system. For example, two distinct contributions to direct current through an open quantum dot due to an oscillating perturbation have been identified[1,2] and observed experimentally in Ref. 3.

In this paper, we investigate the statistical properties of dc currents resulting from an applied ac electric field over a wide range of excitation frequencies, paying particular attention to the presence or absence of symmetry with respect to magnetic field in various regimes. Theoretical analysis is based on recently developed time-dependent random matrix theory.[4,5] Experiments use a gate-defined GaAs quantum dot subject to ac excitation of a gate at MHz to GHz frequencies. At low excitation frequencies $\omega \ll \tau_d^{-1}$ (τ_d is the electron dwell time in the dot) the present theoretical results are consistent with those obtained by adiabatic approximations.[1,6] However, the analysis is applicable over a wider range of frequencies $\hbar\omega \lesssim E_T$, where $E_T = \hbar/\tau_{\rm cross}$ is the Thouless energy and $\tau_{\rm cross}$ is the electron crossing time of the dot. At $\hbar\omega \gtrsim E_T$, the system may be studied by methods developed for disordered bulk conductors.[7,8]

Three distinct contributions to dc current through the dot can be identified, resulting from: (i) an applied dc bias; (ii) an ac bias at the excitation frequency (i.e., rectification effects[2]); and (iii) photovoltaic effects.[5,9] Although the origins of the rectification and photovoltaic effects are different, these two effects are hard to distinguish in experiment with rectification current being dominant.[10] The purpose of the present Rapid Communication is to describe distinct features between the rectification and photovoltaic effects. We restrict our attention to a one-parameter excitation, noting that while in the adiabatic regime one- and two-parameter excitations affect the system differently,[1] beyond the adiabatic regime, $\omega \gtrsim \tau_d^{-1}$, the differences disappear.[5]

The Hamiltonian of electrons in the dot in the presence of a magnetic flux Φ is represented by a Hermitian $M\times M$ matrix $\hat{H}(t) = \hat{\mathcal{H}}_\Phi + \hat{\mathcal{V}}\cos\omega t$. We assume that electron dynamics in the dot is fully chaotic.[11] Then the time-independent part $\hat{\mathcal{H}}_\Phi$ may be considered as a random realization of a $M\times M$ matrix from a Gaussian unitary ensemble with the mean level spacing δ_1 and $M \sim E_{\rm T}/\delta_1$. Perturbation $\hat{\mathcal{V}}$ is a matrix from a Gaussian orthogonal ensemble characterized by the strength $C_0 = \pi\,{\rm Tr}\hat{\mathcal{V}}^2/M^2\delta_1$. The parameter C_0 determines the energy displacement of an electron state due to the applied perturbation $\hat{\mathcal{V}}$. The contact between the left (right) lead and the dot contains $N_{\rm l}(N_{\rm r})$ open channels, we enumerate channels, α, in the left ($\alpha = 1,\ldots,N_l$) and the right ($\alpha = N_{\rm l}+1,\ldots,N_{\rm ch}$) contacts, $N_{\rm ch} = N_l + N_r$. The corresponding experimental setup is shown in Fig. 1.

The dc current $\overline{I^\Phi}$ through the dot is determined by the scattering matrix $[\mathcal{S}_\Phi(t,t')]_{\alpha\beta}$ (see Ref. 5)

$$\overline{I^\Phi} = \frac{e\omega}{2\pi}\int_0^{2\pi/\omega} dt \int_{-\infty}^{+\infty} dt_1 dt_2 \times {\rm Tr}\{\hat{f}(t_1,t_2)[\hat{\mathcal{S}}^\dagger_\Phi(t_2,t)\hat{\Lambda}\hat{\mathcal{S}}_\Phi(t,t_1) - \hat{\Lambda}\delta_{t,t_1}\delta_{t,t_2}]\}. \quad (1)$$

Here $\delta_{t,t'} = \delta(t-t')$ and

$$f_{\alpha\beta}(t,t') = \frac{k_{\rm B}T}{\hbar}\frac{\delta_{\alpha\beta}\exp\left[i\frac{e}{\hbar}\int_{t'}^{t} V_\alpha(\tau)d\tau\right]}{\sinh[\pi k_{\rm B}T(t-t')/\hbar]} \quad (2)$$

is the distribution function of electrons in channel α at temperature T and voltage $V_\alpha(t)$. At sufficiently low frequencies $\omega \ll E_c/\hbar$ (E_c is the dot charging energy) $V_\alpha(t)$ is simply related to the bias $V(t)$ across the dot: $V_\alpha(t) = \Lambda_{\alpha\alpha}V(t)$. Elements of the diagonal matrix $\hat{\Lambda}$ are $\Lambda_{\alpha\alpha} = N_{\rm r}/N_{\rm ch}$ for $1 \leqslant \alpha \leqslant N_l$, and $\Lambda_{\alpha\alpha} = -N_{\rm l}/N_{\rm ch}$ for $N_l < \alpha \leqslant N_{\rm ch}$.

We consider the bias $V(t)$ across the dot in the form $V(t) = V_0 + V_\omega\cos(\omega t + \varphi_1)$. The dc current through the dot to first order in dc bias V_0 and ac bias V_ω is[12]

$$\overline{I^\Phi} = \overline{I^\Phi_{\rm ph}} + \overline{I^\Phi_1} + \overline{g^\Phi_0}V_0, \quad \overline{I^\Phi_1} = \overline{g^\Phi_1}V_\omega, \quad (3)$$

where the first term represents the photovoltaic current $\overline{I^\Phi_{\rm ph}} = \overline{I^\Phi}(V_\alpha \equiv 0)$, see Eqs. (1) and (2). The second and third terms in Eq. (3) represent the contributions to the current due to dc bias V_0 and ac bias V_ω, respectively,

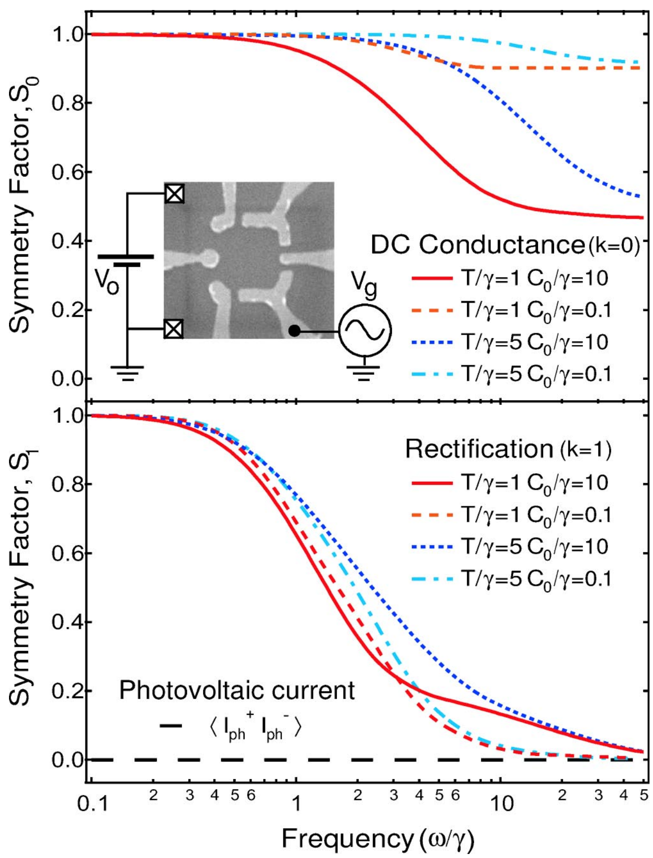

FIG. 1. (Color online) Symmetry factor $S_k = \langle\overline{\delta G_k^{+\Phi}}\;\overline{\delta G_k^{-\Phi}}\rangle/\langle(\overline{\delta G_k^{\Phi}})^2\rangle$ as a function of frequency ω for $k=0$ (upper panel) and $k=1$ (lower panel) at two values of temperature T and power C_0 of the ac excitation. Inset: micrograph of the device and a schematic picture of applied voltages.

$$\overline{g_0^{\Phi}} = \frac{e^2}{\pi\hbar}[G_0 - \overline{\delta G_0^{\Phi}(t)}], \quad \overline{g_1^{\Phi}} = -\frac{e^2}{\pi\hbar}\overline{\delta G_1^{\Phi}(t)}, \tag{4}$$

where $G_0 = N_l N_r / N_{\rm ch}$ is the classical conductance and $\overline{\delta G_k(t)} = \int_0^{2\pi/\omega}\delta G_k(t)\omega dt/2\pi$ stands for time averaging of the "instantaneous conductance" ($k=0$, 1)

$$\delta G_k^{\Phi}(t) = \int d\tau F_k(\tau)\int d\theta \cos(k(\omega\theta + \varphi_k)) \times \mathrm{Tr}\left\{\hat{\Lambda}\hat{\mathcal{S}}_{\Phi}^{\dagger}\left(\theta - \frac{\tau}{2}, t\right)\hat{\Lambda}\hat{\mathcal{S}}_{\Phi}\left(t, \theta + \frac{\tau}{2}\right)\right\},$$

$$F_0(\tau) = \frac{\pi k_B T\tau/\hbar}{\sinh(\pi k_B T\tau/\hbar)}, \quad F_1(\tau) = \frac{2\pi k_B T \sin(\omega\tau/2)}{\hbar\omega\sinh(\pi k_B T\tau/\hbar)}. \tag{5}$$

We observe that $\overline{\delta G_1(t)} = \overline{\delta G_0(t)\cos(\omega t + \varphi_1)}$ in the adiabatic limit $\hbar\omega \ll \max\{N_{\rm ch}\delta_1, k_B T\}$ considered in Refs. 2,13.

Below we study the variance of the photovoltaic current $\overline{I^{\Phi}_{\rm ph}}$ and the conductances $\overline{g_0^{\Phi}}$ and $\overline{g_1^{\Phi}}$ with respect to random realizations of the Hamiltonian $\hat{\mathcal{H}}_{\Phi}$. Following Refs. 5 and 14, we find in the limit $N_{\rm ch} \gg 1$ and at magnetic fields $\Phi \gg \Phi_0\sqrt{N_{\rm ch}/M}$ destroying the weak localization ($\Phi_0 = hc/e$)

$$\langle(\overline{I^{\Phi}_{\rm ph}})^2\rangle = \frac{G_0 e^2\omega^4 C_0\delta_1}{2\pi^3\hbar^2}\int_0^{2\pi/\omega}\frac{dtdt'}{4\pi^2}\int_0^{\infty}d\tau\int_{\tau/2}^{\infty}d\theta K^{+}B^{\rm ph}_{t-\theta,t'-\theta;\tau}, \tag{6}$$

$$\langle\overline{\delta G_k^{+\Phi}\,\delta G_k^{\pm\Phi}}\rangle = \frac{G_0^2\omega^2\delta_1^2}{2\pi^2\hbar^2}\int_0^{2\pi/\omega}\frac{dtdt'}{4\pi^2}\int_0^{\infty}d\tau\int_{\tau/2}^{\infty}d\theta\, K^{\pm}B^{(k)}_{t-\theta,t'-\theta;\tau} \tag{7}$$

and $\langle\overline{I^{+\Phi}_{\rm ph}}\,\overline{I^{-\Phi}_{\rm ph}}\rangle = 0$ (see Ref. 6). In Eqs. (6) and (7) the angle brackets $\langle\cdots\rangle$ stand for the averaging with respect to realizations of $\hat{\mathcal{H}}_{\Phi}$. Functions $B^{(k)}_{t,t';\tau}$ and $B^{\rm ph}_{t,t';\tau}$ describe the distribution function[15] of electrons in the dot in the presence of time-dependent electric fields and kernels $K^{\pm} \equiv K^{\pm}_{t,t';\theta,\tau}$ describe the evolution of electron states[16] in these fields. Both functions $B^{(k)}_{t,t';\tau}$ and $B^{\rm ph}_{t,t';\tau}$ and the kernels $K^{\pm}_{t,t';\theta,\tau}$ contain the diffuson $\mathcal{D}(t_1,t_2,\tau) = \exp[-\int_{t_2}^{t_1}\Gamma(\tau,t)dt]$ or the Cooperon $\mathcal{C}(\tau_1,\tau_2,t) = \exp\left[-\left(\frac{1}{2}\right)\int_{\tau_2}^{\tau_1}\Gamma(\tau,t)d\tau\right]$. Here, $\Gamma(\tau,t) = \gamma_{\rm e} + \gamma_{\varphi} + 4C_0\sin^2\omega t\sin^2(\omega\tau/2)$, where $\gamma_{\rm e} = \delta_1 N_{\rm ch}/2\pi$ is the electron escape rate and γ_{φ} is the electron phase relaxation rate due to inelastic processes.

In the experiment, the ac bias V_{ω} results from capacitive coupling between the leads and the gate on which the ac voltage is applied (see the inset in Fig. 1). Therefore V_{ω} is proportional to the amplitude of the ac voltage at the gate. Assuming that C_0 is linear in the applied power to the gates, we write $V_{\omega} = \alpha_{\omega}\sqrt{C_0/\gamma_{\rm e}}$. The coefficient α_{ω} has units of voltage and is independent of realizations of the quantum dot (we disregard fluctuations of $\hat{\mathcal{V}}$ over different realizations of $\hat{\mathcal{H}}_{\Phi}$). Therefore, the correlation functions of the rectification current $\overline{I_1^{\Phi}} = \overline{g_1^{\Phi}}V_{\omega}$ are determined by the correlators of $\overline{\delta G_1^{\Phi}}$

$$\langle\overline{I_1^{+\Phi}}\,\overline{I_1^{\pm\Phi}}\rangle = \frac{e^4}{\pi^2\hbar^2}\alpha_{\omega}^2\frac{C_0}{\gamma_{\rm e}}\langle\overline{\delta G_1^{+\Phi}}\;\overline{\delta G_1^{\pm\Phi}}\rangle. \tag{8}$$

We also notice that in the limit $N_{\rm ch} \gg 1$ the correlation function of the photovoltaic current $\overline{I^{\Phi}_{\rm ph}}$ and the rectification current $\overline{I_1^{\Phi}}$ vanishes:[6] $\langle\overline{I^{\Phi}_{\rm ph}}\;\overline{I_1^{\Phi}}\rangle = 0$.

First we use Eqs. (7) and (8) to analyze the magnetic field symmetry of the rectification current $\overline{I_1^{\Phi}}$. Although in the adiabatic limit $\omega \ll \gamma_{\rm e}/\hbar$ the rectification current $\overline{I_1^{\Phi}}$ is symmetric with respect to magnetic field inversion ($\Phi \to -\Phi$), at higher frequencies $\omega \gtrsim \gamma_{\rm e}/\hbar$ the symmetry of $\overline{I_1^{\Phi}}$ is suppressed. Indeed, the magnetic field symmetry is related to the time inversion symmetry. For a harmonic field at frequency ω, the time-inversion symmetry holds only on time scales much smaller than $1/\omega$. Transport through the system is determined by times of the order of $\hbar/\gamma_{\rm e}$ and consequently the magnetic field symmetry of the rectification current breaks if $\hbar\omega \gtrsim \gamma_{\rm e}$. We plot the ratio $S_1 = \langle\overline{\delta G_1^{+\Phi}}\;\overline{\delta G_1^{-\Phi}}\rangle/\langle(\overline{\delta G_1^{\Phi}})^2\rangle$ as a function of $\hbar\omega/\gamma_{\rm e}$ in Fig. 1. $S_1 = 1$ represents the symmetric current $\overline{I_1^{\Phi}} \propto \overline{\delta G_1^{\Phi}}$ with respect to magnetic field inversion. In the adiabatic regime this symmetry originates from the Onsager symmetry[17] of the dc conductivity (see Eq. (5) and Refs. 2,3). As the frequency increases, S_1 vanishes, signal-

ling the suppression of the magnetic field symmetry. Therefore, the absence of magnetic field symmetry no longer serves as a feature which allows one to distinguish the photovoltaic current $\overline{I^{\Phi}_{\rm ph}}$ from the rectification current $\overline{I^{\Phi}_{1}}$.

We notice that the magnetic field symmetry of the dc conductance $\overline{\delta G^{\Phi}_0}$ is more sturdy than the symmetry of the rectification current (see Fig. 1). Particularly, at temperatures $k_BT \gtrsim \gamma_{\rm e}$, dc conductance $\overline{\delta G^{\Phi}_0}$ is nearly symmetric at frequencies $\hbar\omega \lesssim k_BT$, since the dc correlation function is determined by processes on a time scale $\hbar/k_{\rm B}T$. The symmetry is not fully suppressed even at $\omega \gg k_{\rm B}T/\hbar$; the suppression depends on $C_0/\gamma_{\rm e}$.

We apply Eqs. (6)–(8) to the analysis of the experiment.[3] The quantum dot used in the experiment has an area $A \approx 0.7\ \mu{\rm m}^2$. Relevant energy scales are the Thouless energy $E_T \approx 160\ \mu{\rm eV}$ and the mean level spacing $\delta_1 = \pi\gamma_{\rm e} \approx 10\ \mu{\rm eV}$. The measurements were performed at the base electron temperature $T \approx 200$ mK ($k_{\rm B}T = 5.4\gamma_{\rm e}$). From the size of conductance fluctuations without ac fluctuation on the gate, we estimate the dephasing rate $\gamma_\varphi \approx 0.2\gamma_{\rm e}$ (see Ref. 18 for details) and thus disregard γ_φ and energy relaxation rate $\gamma_\varepsilon \leqslant \gamma_\varphi$ in our quantitative analysis.

In the upper panel of Fig. 2 we show the variance of the conductance as a function of the incident power P at $\omega/2\pi = 5.56$ GHz ($\hbar\omega/\gamma_{\rm e} \approx 7.2$). We also plot the variance of the conductance calculated from Eq. (7) ($k=0$) at temperature $T = 5.4\gamma_{\rm e}/k_{\rm B}$. Assuming that the ratio $C_0/\gamma_{\rm e}$ is proportional to the power P of the ac excitation applied to the gate, i.e., $C_0/\gamma_{\rm e} = P/P_0$, we rescale P to obtain the best fit of the experimental points by the curve of Eq. (7). We find $P_0 = 9 \times 10^{-8}$ W.

In the lower panel of Fig. 2 we show the correlators $\langle \overline{I^{+\Phi}}\,\overline{I^{\pm\Phi}} \rangle$ of the measured current. Although the traces of the magnetic field sweeps (see Fig. 3 in Ref. 3) look quite asymmetric for the measured current, the antisymmetric correlator $\langle \overline{I^{+\Phi}}\,\overline{I^{-\Phi}} \rangle$ is not significantly smaller than its symmetric counterpart. We notice however, that if the averaging is performed over n realizations, the measured correlator $\langle \overline{I^{+\Phi}}\,\overline{I^{-\Phi}} \rangle$ can be estimated as $\langle \overline{I^{+\Phi}}\,\overline{I^{+\Phi}} \rangle/\sqrt{n}$ ($n \sim 50$ in the experiment).

We plot the variance of the photovoltaic current, Eq. (6), as a function of $C_0/\gamma_{\rm e}$ for $k_BT = 5.4\gamma_{\rm e}$ and $\hbar\omega = 7.2\gamma_{\rm e}$ (to facilitate numerics, we used the approximation $\hbar\omega \gg \gamma_{\rm e}$). We emphasize that the horizontal shift between the data points and curve is fixed by the fit in the upper panel for the dc conductance and there are no fitting parameters for the variance of the current (along the vertical axis). At $C_0 \lesssim \gamma_{\rm e}$, the variance of the measured current changes quadratically in $C_0/\gamma_{\rm e}$, consistent with quadratic dependence on C_0 of the theoretical curves for $\langle \overline{I^2_{\rm ph}} \rangle$ and therefore our assumption that C_0 is proportional to the power of the ac excitation is justified. At $C_0 \gtrsim \gamma_{\rm e}$ the variance of the measured current starts saturating. This saturation is expected for large power asymptote of the photovoltaic current due to the spreading of the distribution function of electrons in the dot.[5] Some deviation between the experimental points and the theoretical curve is expected due to the approximation $N_{\rm ch} \gg 1$ used for derivation of Eq. (6) ($N_{\rm ch} = 2$ in the experiment).

For illustration, we also plot the correlation functions of the rectification current, using Eq. (8) for $\varphi_1 = 0$ and $\alpha_\omega = 0.45\hbar\omega/e$. For the rectification current, the saturation at large power is not expected: according to Fig. 2, $\langle \overline{I^{+\Phi}_1}\,\overline{I^{\pm\Phi}_1} \rangle \propto (C_0/\gamma_{\rm e})^a$ with $a \approx 0.6$.

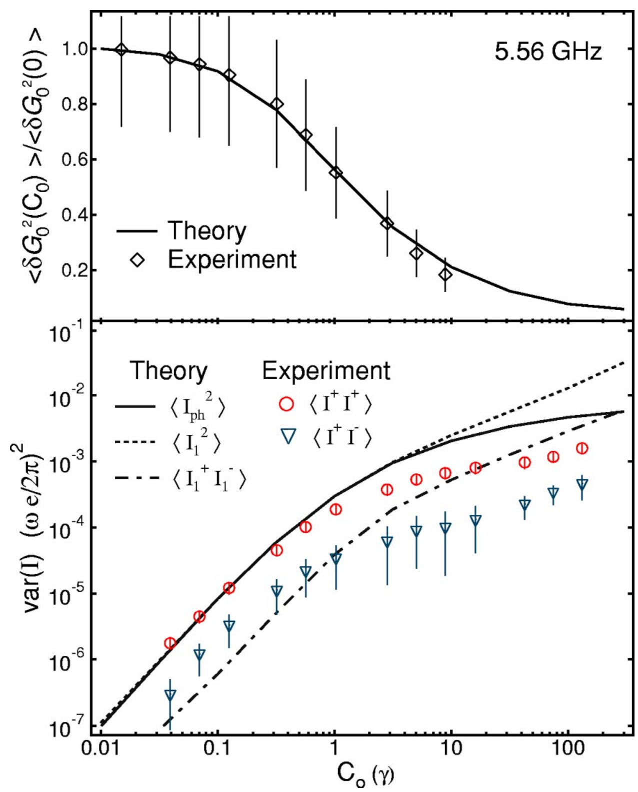

FIG. 2. (Color online) Upper panel: Variance of the conductance as a function of the ac excitation power $P = P_0C_0/\gamma_{\rm e}$ at $\omega/2\pi = 5.56$ GHz ($\hbar\omega = 7.2\gamma_{\rm e}$) and the theoretical result of Eq. (7) with $k=0$. We use $P_0 = 9 \times 10^{-8}$ W and $k_BT = 5.4\gamma_{\rm e}$. Lower panel: Symmetric (solid triangles) and antisymmetric (open triangles) current correlators as a function of ac excitation strength C_0. The solid line shows the variance of the photovoltaic current Eq. (6) with parameters fixed by the fit in the upper panel. The dashed and dotted lines show the symmetric and antisymmetric correlators of the rectification current Eq. (8) with $\alpha_\omega = 0.45\hbar\omega/e$ and $\varphi_1 = 0$.

We similarly discuss the data for $\omega/2\pi = 2.4$ GHz. Performing the fit of the experimental values of the conductance fluctuations and the result of Eq. (7) with $k=0$ and temperature $T = 5.4\gamma_{\rm e}/k_B$, we find the relation between the strength of the perturbation C_0 and the power $P = P_0C_0/\gamma_{\rm e}$ with $P_0 = 2.5 \times 10^{-7}$ W.

In Fig. 3 we show the symmetric and antisymmetric current correlators for 2.4 GHz. For comparison we plot by a solid line the variance of the photovoltaic current $\overline{I^{\Phi}_{\rm ph}}$, calculated from Eq. (6) at $\hbar\omega = 3.1\gamma_{\rm e}$. We observe that the fluctuations of the measured current significantly exceed (by a factor ~ 100) the expected magnitude for the photovoltaic current, and therefore are likely due to the rectification of the bias across the dot. The low power data can be fitted by Eq. (8) with $\alpha_\omega = 4.7\hbar\omega/e$.

The above choice for $\alpha_\omega \gtrsim \{\hbar\omega, k_BT\}/e$ limits the applicability of the linear expansion Eq. (3) to small powers of the ac excitation C_0, such that $C_0/\gamma_{\rm e} \lesssim (\hbar\omega/e\alpha_\omega)^2$. The higher order corrections in the bias V_ω do not restore magnetic field

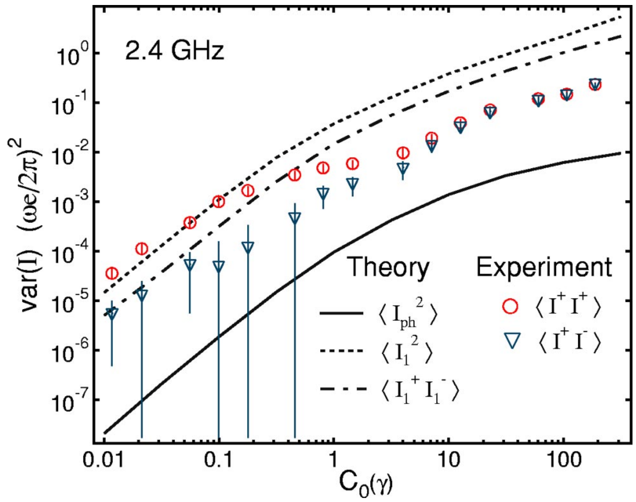

FIG. 3. (Color online) Symmetric (solid triangles) and antisymmetric (open triangles) current correlators at $\omega/2\pi=2.4$ GHz as a function of power $P=P_0C_0/\gamma_e$, with $P_0=2.5\times10^{-7}$ W. The solid line shows the variance of the photovoltaic current Eq. (6) at temperature $T=5.4\gamma_e/k_B$ and frequency $\omega=3.1\gamma_e/\hbar$. The dashed and dotted lines show the symmetric and antisymmetric correlators of the rectification current Eq. (8) with $\alpha_\omega=4.7\hbar\omega/e$ and $\varphi_1=0$.

symmetry, which is in apparent contradiction to the observed symmetry of the measured current at larger powers (at $C_0/\gamma_e \gtrsim 1$ in Fig. 3). We attribute the restoration of magnetic field symmetry to dephasing due to dot heating by the dissipative current. Increasing the power P at fixed ω drives the system into the adiabatic regime since the heating makes the ratio $\hbar\omega/(\gamma_e+\gamma_\varphi)$ decrease. As shown in Fig. 1, the rectification current is symmetric in the adiabatic regime. The assumption that γ_φ increases as power P increases is consistent with the observed change of the correlation field for the current fluctuations. Indeed, according to Fig. 4 in Ref. 3, as the power changes from 10 to 10^4 nW, $\gamma_e+\gamma_\varphi$ increases by factor of 4 and becomes larger than $\hbar\omega$. In this regime the rectification current is mostly symmetric with respect to magnetic field inversion (see Fig. 1).

In summary, we studied ensemble fluctuations of dc current through an open quantum dot subject to oscillating perturbation. We showed that as frequency of the perturbation increases, magnetic field symmetry of the current disappears, regardless of the mechanism of the current generation. We demonstrated that the power behavior of the current fluctuations is an important tool to distinguish effects of an ac excitation on dc current.

We thank I. Aleiner, P. Brouwer, and V. Falko for useful discussions, C. I. Duruöz and J. S. Harris, Jr. for high-quality heterostructure materials, and S. M. Patel for device fabrication. The work was supported by NSF Grants No. DMR 02-13282, DMR 0072777, DMR 0408638 and by AFOSR Grant No. F49620-01-1-0475.

*Present address: Department of Applied Physics, Yale University, New Haven, CT 06520.

[1] P. W. Brouwer, Phys. Rev. B **58**, R10135 (1998).
[2] P. W. Brouwer, Phys. Rev. B **63**, 121303(R) (2001).
[3] L. DiCarlo, C. M. Marcus, and J. S. Harris, Phys. Rev. Lett. **91**, 246804 (2003).
[4] M. G. Vavilov and I. L. Aleiner, Phys. Rev. B **60**, R16311 (1999).
[5] M. G. Vavilov, V. Ambegaokar, and I. L. Aleiner, Phys. Rev. B **63**, 195313 (2001).
[6] T. A. Shutenko, I. L. Aleiner, and B. L. Altshuler, Phys. Rev. B **61**, 10366 (2000).
[7] B. L. Altshuler *et al.*, *Quantum Theory of Solids* (Mir Publisher, Moscow, 1982).
[8] X.-B. Wang and V. E. Kravtsov, Phys. Rev. B **64**, 033313 (2001).
[9] V. I. Falko and D. E. Khmel'nitskii, Zh. Eksp. Teor. Fiz. **95**, 328, (1989) [Sov. Phys. JETP **68**, 186 (1989)].
[10] H. Linke, W. Sheng, A. Löfgren, Hongqi Xu, P. Omling, and P. E. Lindelof, Europhys. Lett. **44**, 341 (1998); H. Linke, T. E. Humphrey, P. E. Lindelof, A. Löfgren, R. Newbury, P. Omling, A. O. Sushkov, R. P. Taylor, and H. Xu, Appl. Phys. A **75**, 237 (2002).
[11] Alternative methods to the time-dependent random matrix theory here are based on the Floquet approach [see M. Moskalets and M. Büttiker, Phys. Rev. B **66**, 205320 (2002)], or a time-dependent scattering matrix approach [see M. L. Polianski and P. W. Brouwer, J. Phys. A **36**, 3215 (2003)].
[12] The biased current produces heating and the analysis beyond the linear response in the bias voltage requires consideration of heat relaxation in the system.
[13] M. Moskalets and M. Büttiker, Phys. Rev. B **69**, 205316 (2004).
[14] M. G. Vavilov and I. L. Aleiner, Phys. Rev. B **64**, 085115 (2001).
[15] $B^{(k)}_{t,t';\tau}=F_k^2(\tau)\cos[k(\omega t+\varphi_k)]\cos[k(\omega t'+\varphi_k)]$ and $B^{\mathrm{ph}}_{t,t';\tau}=(\gamma_e/\hbar)^2F_1^2(\tau)\int_0^\infty d\xi d\xi'\mathcal{D}(t,t-\xi,\tau)\mathcal{D}(t',t'-\xi',\tau)\times[\sin\omega t\sin\omega t'+(2C_0/\gamma_e)\sin^2\omega(t-\xi)\sin^2\omega(t'-\xi')\sin^2(\omega\tau/2)]$.
[16] $K^+_{t,t';\theta,\tau}=\mathcal{D}((t+t')/2,(t+t'+\tau)/2-\theta,t'-t)\mathcal{D}((t+t')/2,(t+t'-\tau)/2-\theta,t-t')$ and $K^-_{t,t';\theta,\tau}=\mathcal{C}(t-t'+\theta-\tau/2,t-t'-\theta+\tau/2,(t+t'-\theta)/2+\tau/4)\times\mathcal{C}(t'-t+\theta+\tau/2,t'-t-\theta-\tau/2,(t+t'-\theta)/2-\tau/4)$.
[17] L. Onsager, Phys. Rev. **38**, 2265 (1931); M. Büttiker, Phys. Rev. Lett. **57**, 1761 (1986).
[18] A. G. Huibers, J. A. Folk, S. R. Patel, C. M. Marcus, C. I. Duruöz, and J. S. Harris, Jr., Phys. Rev. Lett. **83**, 5090 (1999).